Plant Science 335 (2023) 111797

Contents lists available at ScienceDirect

Plant Science

journal homepage: www.elsevier.com/locate/plantsci

Comparative analysis of the Squamosa Promoter Binding-Like (SPL) gene family in *Nicotiana benthamiana* and *Nicotiana tabacum*

Carmine De Paola [a], Victor Garcia-Carpintero [a], Marta Vazquez-Vilar [a], Kacper Kaminski [b], Asun Fernandez-del-Carmen [a], Nicolas Sierro [b], Nikolai V. Ivanov [b], Giovanni Giuliano [c], Peter Waterhouse [d], Diego Orzaez [a,*]

[a] *Instituto de Biología Molecular y Celular de Plantas (CSIC-UPV), Valencia, Spain*
[b] *PMI R&D, Philip Morris Products S.A, Neuchâtel, Switzerland*
[c] *ENEA, Casaccia Research Center, Rome, Italy*
[d] *Queensland University of Technology, Brisbane, Australia*

ARTICLE INFO

Keywords:
Plant biofactories
Nicotiana benthamiana
Tobacco
SQUAMOSA PROMOTER BINDING-LIKE
CRISPR/Cas9
Flowering time

ABSTRACT

SQUAMOSA PROMOTER BINDING-LIKE (SPL) proteins constitute a large family of transcription factors known to play key roles in growth and developmental processes, including juvenile-to-adult and vegetative-to-reproductive phase transitions. This makes SPLs interesting targets for precision breeding in plants of the *Nicotiana* genus used as e.g. recombinant biofactories. We report the identification of 49 *SPL* genes in *Nicotiana tabacum* cv. K326 and 43 *SPL* genes in *Nicotiana benthamiana* LAB strain, which were classified into eight phylogenetic groups according to the SPL classification in *Arabidopsis*. Exon-intron gene structure and DNA-binding domains were highly conserved between homeologues and orthologues. Thirty of the *NbSPL* genes and 33 of the *NtSPL* genes were found to be possible targets of microRNA 156. The expression of *SPL* genes in leaves was analysed by RNA-seq at three different stages, revealing that genes not under miR156 control were in general constitutively expressed at high levels, whereas miR156-regulated genes showed lower expression, often developmentally regulated. We selected the *N. benthamiana SPL13_1a* gene as target for a CRISPR/Cas9 knock-out experiment. We show here that a full knock-out in this single gene leads to a significant delay in flowering time, a trait that could be exploited to increase biomass for recombinant protein production.

1. Introduction

SQUAMOSA PROMOTER BINDING-LIKE PROTEINs (*SPL*) is a family of plant-specific transcription factors. *SPL* genes control many aspects of plant development and physiology, including vegetative phase transition (Xu et al., 2016), flowering time (Gandikota et al., 2007; Xu et al., 2016), leaf initiation rate and shoot and inflorescence branching (Schwarz et al., 2008; Wu and Poethig, 2006), fruit development and ripening (Ferreira e Silva et al., 2014), floral organ development and fertility (Xing et al., 2010), pollen sac development (Unte et al., 2003), trichome development (Yu et al., 2010), root development (Yamasaki et al., 2009; Yu et al., 2015), and stress responses (Mao et al., 2016; Zeng et al., 2019). The first two *SPL* genes were discovered in *Antirrhinum majus* and were named SQUAMOSA PROMOTER BINDING PROTEIN (AmSBP1 and AmSBP2) due to their in vitro binding activity with the promoter of the floral meristem identity gene SQUAMOSA (Klein et al., 1996). After this discovery, *SPL* genes were found in green algae, mosses, gymnosperms, and angiosperms (Preston and Hileman, 2013).

Proteins belonging to the SPL family are characterized by the presence of the SBP domain, a DNA binding domain of approximately 78 amino acid residues. This domain contains two zinc-finger motifs, Cys–Cys–Cys–His (Zn1) and Cys–Cys–His–Cys (Zn2), with the second motif partially overlapping a nuclear localization signal at the C-terminal of the SBP domain (Birkenbihl et al., 2005; Cardon et al., 1999). Additionally, some *SPL* genes contain conserved microRNA 156 (miR156) binding sites. MicroRNAs are non-coding RNAs that can complementarily bind to target sites and repress expression via mRNA cleavage or repression of translation (Rogers and Chen, 2013). The

Abbreviations: SPL, SQUAMOSA promoter binding-like; miRNA, micro RNA; CRISPR, Clustered Regularly Interspaced Short Palindromic Repeats; Cas9, CRISPR associated protein 9.

* Correspondence to: Instituto de Biología Molecular y Celular de Plantas (CSIC-UPV), C/ de l'Enginyer Fausto Elio, s/n, 46011 Valencia, Spain.
E-mail address: dorzaez@ibmcp.upv.es (D. Orzaez).

https://doi.org/10.1016/j.plantsci.2023.111797
Received 27 March 2023; Received in revised form 14 July 2023; Accepted 16 July 2023
Available online 17 July 2023

miR156 complementary sites are present in the coding region or in the 3' untranslated region (3'-UTR) of several *SPL* genes. Numerous studies confirmed that the level of miR156 is responsible for phase transitions in plants - MiR156 accumulates at high levels at seedling stage and during the juvenile phase, while its amount is significantly reduced in the adult phase (Xu et al., 2016; T. Zhang et al., 2015). In parallel to the decrease of miR156 levels, the expression level of miR156-targeted *SPLs* rises with age, ultimately leading to the reproductive phase transition (H. Wang and Wang, 2015).

The specific role of each *SPL* gene in the plant has been extensively studied in *Arabidopsis thaliana*. *Arabidopsis* possesses 16 *SPL* genes (Cardon et al., 1999). These can be divided in eight clades: *AtSPL1/12/14/16, AtSPL2/10/11, AtSPL3/4/5, AtSPL6, AtSPL7, AtSPL8, AtSPL9/15*, and *AtSPL13* (Preston and Hileman, 2013; Z. Yang et al., 2008). In *Arabidopsis*, 10 out of the 16 *SPL* genes are targets of miR156 (Gandikota et al., 2007; Wu & Poethig, 2006). Among the ones regulated by miR156, *AtSPL2/9/10/11/13/15* contribute to both the juvenile-to-adult phase transition (vegetative phase change) and the vegetative-to-reproductive phase transition (reproductive phase change or flowering), with *AtSPL9/13/15* being more important than *AtSPL2/10/11* (Xu et al., 2016). *AtSPL3/4/5* do not play a major role in vegetative phase change or flowering but promote the floral meristem identity transition (Xu et al., 2016). *AtSPL6* does not have a major function in vegetative morphogenesis (Xu et al., 2016), but it can positively regulate a subset of defence genes and plays a role in effector-triggered immunity (Padmanabhan et al., 2013). Among the ones not regulated by miR156, *AtSPL7* is a central regulator of copper homeostasis and plays a major role in cadmium response (Gielen et al., 2016; Yamasaki et al., 2009), *AtSPL8* plays pivotal roles in regulating pollen sac development, male fertility, and gibberellin (GA) biosynthesis and signalling (Unte et al., 2003; Xing et al., 2010; Y. Zhang et al., 2007) and *AtSPL14* regulates plant development and sensitivity to fumonisin B1 (Stone et al., 2005).

Genome-wide analyses of the *SPL* gene family were performed in many plant species other than *Arabidopsis* (Cardon et al., 1999), including rice (Z. Yang et al., 2008), maize (Mao et al., 2016), cotton (Cai et al., 2018), barley (Tripathi et al., 2018), tomato (Salinas et al., 2012), citrus (Zeng et al., 2019), poplar (Li and Lu, 2014), Chrysanthemum (Song et al., 2016), Moso Bamboo (Pan et al., 2017), Petunia (Zhou et al., 2018) and Tartary Buckwheat (Liu et al., 2019). In tobacco, there is one report in which Han et al. identified and characterized 15 *SPL* genes in *N. tabacum* L. cv. Qinyan95 (Han et al., 2016). However, a genome-wide identification of *SPL* genes in the plants of the Nicotiana genus is not available.

Nicotiana benthamiana and *Nicotiana tabacum* are two plant species of the Nicotiana genus with suitable properties to be engineered into efficient biofactories for high value-added compounds production (Derevnina et al., 2019; Goodin et al., 2008; Sierro et al., 2014). Both species have a high metabolic versatility and a non-food status. Moreover, several biotechnological tools have been developed for their genetic manipulation. Among others, transient recombinant gene expression via Agroinfiltration is widely used for research and bioproduction purposes as it results in high yields of recombinant protein in both species. As an initial step towards exploiting the potential of *SPL* targeted mutagenesis for the breeding of *N. tabacum* and *N. benthamiana* biofactories, we reported in this study the genome-wide identification and characterization of the *SPL* genes in *N. benthamiana* LAB strain and in *N. tabacum* cv. K326. We identified 49 (48 with SBP) putative *SPL* genes in *N. tabacum* cv. K326. The high quality of the recently released new version of the *N. benthamiana* genome (Ranawaka et al., 2022) also allowed us to identify 43 (37 with SBP) candidate *SPL* genes in *N. benthamiana* LAB strain. Additionally, we analysed the gene structure, conserved motifs, and expression profile of the identified *SPLs*. We also described how the CRISPR/Cas9-directed knock out of a single gene in the smallest *SPL* subfamily in *N. benthamiana*, the *SPL13* clade comprising three genes (only one with SBP), leads to a consistent delay of flowering initiation time of approximately five days, a change that could impact production yields.

2. Materials and methods

2.1. Search of SPL genes in N. benthamiana and N. tabacum cv. K326

SPL families from *Arabidopsis thaliana* (TAIR10), *Solanum lycopersicum, Nicotiana tomentosiformis* and *Nicotiana sylvestris* were retrieved and protein sequences were used to search for homologs in the *N. benthamiana* (LAB330, version 3.02 https://www.nbenth.com/) (Nicotiana benthamiana Genome & Wild Transcriptome Site, n.d.; Ranawaka et al., 2022) and *N. tabacum* cv. K326 (Nitab v4.5 Genome Scaffolds Edwards 2017, https://solgenomics.net/tools/blast/) (Edwards et al., 2017) reference genomes using TBLASTN. Matches with a 50% identity and 50% of coverage were checked for annotated gene models. Gene models were aligned to the National Center for Biotechnology Information (NCBI) non-redundant protein sequences database (Sayers et al., 2022) using BLASTP (Altschul et al., 1990). Gene models with top matches against annotated SPL proteins were kept as *N. benthamiana* and *N. tabacum* cv. K326 SPL family members. In order to verify the completeness of the SPLs search for both *N. benthamiana* and *N. tabacum* cv. K326, the smallest SPL member of each species was selected and aligned against all protein sequences for each genome using BLASTP.

2.2. Reannotation of N. tabacum cv. K326 SPLs members

SPLs identified for *N. tabacum* cv. K326 were aligned to the NBCI non-redundant protein sequence dataset (Sayers et al., 2022) using BLASTP (Altschul et al., 1990). For each one, the top match originating from *N. tabacum*, *N. sylvestris* or *N. tomentosiformis* was selected, using NCBI's RefSeq curated gene models when possible and compared with K326 gene models. If either number of exons and/or sequence length was different, a new gene model for K326 was searched with Exonerate V2.2 (Slater and Birney, 2005), using the protein from NCBI as query and the K326 source scaffold (Edwards et al., 2017) or the sequences obtained from the updated version (publically not available) of the *N. tabacum* reference genome as target for the new model. Updated *SPL* gene models are listed in Table S2. If the new gene model couldn't fit neither in K326 scaffold nor in the updated version of the *N. tabacum* reference genome, the Nitab v4.5 original model was kept. New gene models were verified with RNA-seq expression data from Solgenomics by visual inspection. Finally, subgenome donors for *N. tabacum* cv. K326 SPL sequences were assigned by BLASTP against NCBI non-redundant protein database.

2.3. Identification of SBP conserved domains and motif analysis

Identified SPL protein sequences from both *N. benthamiana* and *N. tabacum* cv. K326 were scanned for SBP domains using MOTIF Search (https://www.genome.jp/tools/motif/) (MOTIF: Searching Protein Sequence Motifs, n.d.) with default parameters. The conserved motifs along SPL protein sequences were detected by MEME software (http://meme.nbcr.net/meme/cgibin/meme.cgi) and SBP sequence visualization was performed using multiple alignment program MAFFT version 7 (http://mafft.cbrc.jp/alignment/server/; (Katoh et al., 2019)).

2.4. Gene structure and miRNA156 complementary regions

For *N. benthamiana,* coding sequences (CDS) and 3' untranslated regions (3'-UTRs) were retrieved from *N. benthamiana* LAB330 v3.02 gene models. For *N. tabacum* cv. K326, CDS sequences from the old and new gene models were aligned against Nitab v4.5 Genome Scaffolds Edwards 2017 (https://solgenomics.net/tools/blast/) (Edwards et al., 2017), retrieving 5000 bp downstream of the CDS. Both CDS sequences

and downstream sequences were scanned for miRNA156-complementary regions using a *N. tabacum* miRNA database with psRNATarget (Dai et al., 2018) and default parameters. MiR156 binding sites found in the CDS were kept for both species. All miR156 matches in the 3'UTRs from *N. benthamiana* were also kept, while for *N. tabacum* cv. K326 matches farther than 500 bp downstream the CDS were discarded. Browser Extensible Data (BED) files containing *SPL* genes models for each *Nicotiana* species were created with an in-house python script, manually adding 500 bp UTRs windows to *N. tabacum* cv. K326 gene models. These files were graphically represented using GSDS (Gene Structure Display Server) (http://gsds.cbi.pku.edu.cn/).

2.5. Phylogenetic tree and family classification

A multiple sequence alignment (MSA) between *A. thaliana*, *N. benthamiana* and *N. tabacum* cv. K326 SPL protein sequences was performed with MUSCLE v3.8.31 (Edgar, 2004). A phylogenetic tree was constructed with iqtree v1.6.12 (Nguyen et al., 2015) using model VT+F+R4 and a bootstrap value of 1000. All SPLs were named according to the *A. thaliana* TAIR10 *SPL* gene belonging to the same clade. Then, in *N. tabacum* cv. K326 the average protein length for each pair in the clade was calculated, number 1 was assigned to the pair with the highest value, number 2 to the following, and so on. Each pair member was marked as "a" if the most likely subgenome donor was *N. sylvestris* and "b" if it was *N. tomentosiformis*. *N. benthamiana* members were named considering their phylogenetic relationship to *N. tabacum* cv. K326 SPLs: if named with "a" or "b" the most similar subgenome is the *N. sylvestris* or *N. tomentosiformis*, respectively, but if named with "x" or "y" a similar subgenome could not be established, with "x" indicating one donor and "y" another one. Additionally, genes not having a partner were named with an "U", standing for "unique".

2.6. Plant material, growing conditions and samples collection for RNA extraction

N. benthamiana LAB strain and *N. tabacum* cv. K326 plants were grown under a 16-h light (24ºC)/8-h dark (20ºC) regime. For *N. benthamiana*, the whole fifth true leaf from the main axis was collected. Three biological replicates were made, each of them coming from a pool of three leaves. Samples were collected at 4 weeks (Juvenile stage: J), 5 weeks (Pre-flowering stage: P), 6 weeks (Flowering stage: F). For *N. tabacum* cv. K326, the whole fifth true leaf was collected at 60 days (J), 75 days (P), 100 days (F). Three biological replicates were made, each of them coming from an individual plant.

2.7. N. benthamiana phenotyping

For each plant, the day (post sowing) in which the first flower bud was visible was registered, and considered as flowering time. Regarding branching, the lateral branches of each plant were counted, a first time when WT plants flowered, and a second time, when each SPL13-edited plant flowered. All secondary growth axes, including nascent axillary meristems, emerging from the main axis were recorded as lateral branches.

2.8. RNA extraction and sequencing

Leaf samples were ground in liquid nitrogen and stored at − 80 °C. RNA was extracted with GeneJET RNA purification kit from Thermofisher (USA) following the manufacturer instructions. Extracted RNA samples were prepared with Universal Plus mRNA-Seq with NuQuant. Libraries were later sequenced with an Illumina NovaSeq® 6000 System. Paired end (PE) 2x150bp sequencing was performed with NovaSeq6000 - Dual Index - Paired End - S4 - XP protocol. Sequencing data generated was demultiplexed by Illumina BaseSpace® Clarity LIMS (© Illumina, Inc., USA).

2.9. Expression analysis

Sequence reads were quality checked using FastQC v. 0.11.9 (https://www.bioinformatics.babraham.ac.uk/projects/fastqc/). Raw reads were quality trimmed and Illumina adaptors were removed with Trimmomatic version 0.39 (Bolger et al., 2014). Next, HISAT2 v2–2.2.1 (Kim et al., 2019) was used for mapping the reads. *N. benthamiana* and *N. tabacum* reads were aligned against the *N. benthamiana* genome, version 3.3, (https://www.nbenth.com/) (Nicotiana benthamiana Genome & Wild Transcriptome Site, n.d.; Ranawaka et al., 2022) and against the *N. tabacum* genome, version Nitab v4.5, available at Solgenomics (https://solgenomics.net/organism/Nicotiana_tabacum/genome) (Edwards et al., 2017), respectively. Transcript abundances were calculated for *N. benthamiana* considering annotated gene models v3.02 (Ranawaka et al., 2022) while for *N. tabacum* cv. K326 considering annotated gene models version Nitab v4.5 (Edwards et al., 2017) and using StringTie 2.1.6 (Pertea et al., 2015). From these counts a gene expression table of raw read counts was generated. Genes from this table were filtered out if expression was not found for each development stage. Then, expression levels were normalized by trimmed mean of M-values with EdgeR (Robinson et al., 2010) and an expression table in CPM units was generated.

2.10. Plasmid assembly

Constructs used for transformation were assembled using GoldenBraid (Vazquez-Vilar et al., 2020, 2021). For the assembly of guide RNAs on level 0, two partially complementary primers were designed at https://gbcloning.upv.es/do/crispr/multi_cas9_gRNA_domesticator_1 using as input the sequences of Table S1. Primers were included in a BsmBI restriction–ligation reaction together with pUPD2 and the corresponding level − 1 tRNA-scaffold plasmid (GB1208 for sgSPL1.5 and GB1207 for sgSPL1.6). Later, multipartite *Bsa*I restriction–ligation reactions from level 0 parts and binary *Bsa*I or BsmBI restriction–ligation reactions were performed to obtain all the level $\geq$ 1 assemblies. All plasmids were validated by restriction enzyme (RE) analysis. The sequences of all level $\geq$ 1 constructs can be found entering their IDs (displayed at Table S3) at https://gbcloning.upv.es/search/features/.

2.11. Plant material and genetic transformation

The *N. benthamiana* LAB strain was used for transformation with *Agrobacterium tumefaciens* following a standard protocol (Horsch et al., 1985). Briefly, fully expanded leaves of WT plants were sterilized with 5% commercial bleach for 10 min followed by four consecutive washing steps with sterile deionised water. Leaf discs (d= 0.8 cm) were cut with a cork borer and incubated overnight in co-culture plates (4.9 g/L MS supplemented with vitamins (Duchefa, The Netherlands https://www.duchefa-biochemie.com/), 3% sucrose (Sigma-Aldrich, USA, https://www.sigmaaldrich.com/), 0.8% Phytoagar (Duchefa, The Netherlands), 1 mg/L BAP (Sigma-Aldrich, USA), 0.1 mg/L NAA (Sigma-Aldrich, USA), pH= 5.7). Leaf discs were incubated for 15 min with a culture of *A. tumefaciens* LBA4404 harboring plasmid GB3298 (OD600 =0.3). Discs were returned to the co-cultivation plates and incubated for 2 days in darkness. Next, discs were transferred to selection medium (4.9 g/L MS supplemented with vitamins (Duchefa, The Netherlands), 3% sucrose (Sigma-Aldrich, USA), 0.8% Phytoagar (Duchefa, The Netherlands), 1 mg/L BAP (Sigma-Aldrich, USA), 0.1 mg/L NAA (Sigma-Aldrich, USA), 500 mg/L carbenicillin, 100 mg/L kanamycin, pH= 5.7). Discs were transferred to fresh medium every seven days until shoots appeared (4–6 weeks). Shoots were cut and transferred to rooting medium (4.9 g/L MS supplemented with vitamins (Duchefa, The Netherlands), 3% sucrose (Sigma-Aldrich, USA), 0.8% Phytoagar (Duchefa, The Netherlands), 500 mg/L carbenicillin, 100 mg/L kanamycin, pH= 5.7) until roots appeared.

Transient expression asssays were performed as described in

Moreno-Giménez et al. (2022) with minor differences. Five weeks old *N. benthamiana* WT and NbSPL13_1a/1a/1b/1b (biallelic mutation for both homeologous genes) were used for Agroinfiltration. Bacterial suspensions were adjusted to an optical density of 0.05 at 600 nm (OD600). For enhanced GFP (eGFP) expression with the TMV-based expression system ICON (Giritch et al., 2006), the bacterial suspensions harboring the MagnICON® Integrase (pICH14011), the MagnICON® 5' module (pICH17388) and the 3' eGFP module (GB4294, eGFP cloned in a vector adapted for *Bsa*I cloning from MagnICON® pICH7410 (Diego-Martin et al., 2020)) were mixed in equal volumes. For eGFP expression with a geminiviral replicon system based on the Bean Yellow Dwarf Virus (BeYDV) (Dahan-Meir et al., 2018), equal volumes of bacterial suspensions harbouring plasmids GB3598 and GB4312 were mixed. Leaf samples were collected at 4 and 7 days post infiltration (dpi). For the determination of fluorescence, 0.5 cm diameter disc were excised from Agroinfiltrated leaves and transferred to a black 96-well microplate. Subsequently, enhanced GFP (eGFP) fluorescence was determined using microplate reader Victor™ X5 (Perkin Elmer, USA) following the manufacturer instructions.

2.12. Genomic DNA extraction and editing efficiency evaluation

150 mg of leaf material was used for genomic DNA extraction with the CTAB (cetyl trimethylammonium bromide) method (Murray & Thompson, 1980). The genomic regions flanking the nuclease target sites were PCR amplified using MyTaq™ DNA Polymerase (Bioline, https://www.bioline.com/) and primers listed on Table S4. The PCR amplicons were confirmed on a 1% agarose gel electrophoresis and purified with ExoSAP-IT™ PCR Product Cleanup Reagent (ThermoFisher Scientific, https://www.thermofisher.com) following the manufacturer's indications prior to Sanger sequencing. Chromatograms of Cas9-edited genomic DNA were analyzed using Inference of CRISPR Edits (ICE) v2 tool from Synthego (https://ice.synthego.com/) (Synthego, n.d.). All analyses were manually curated.

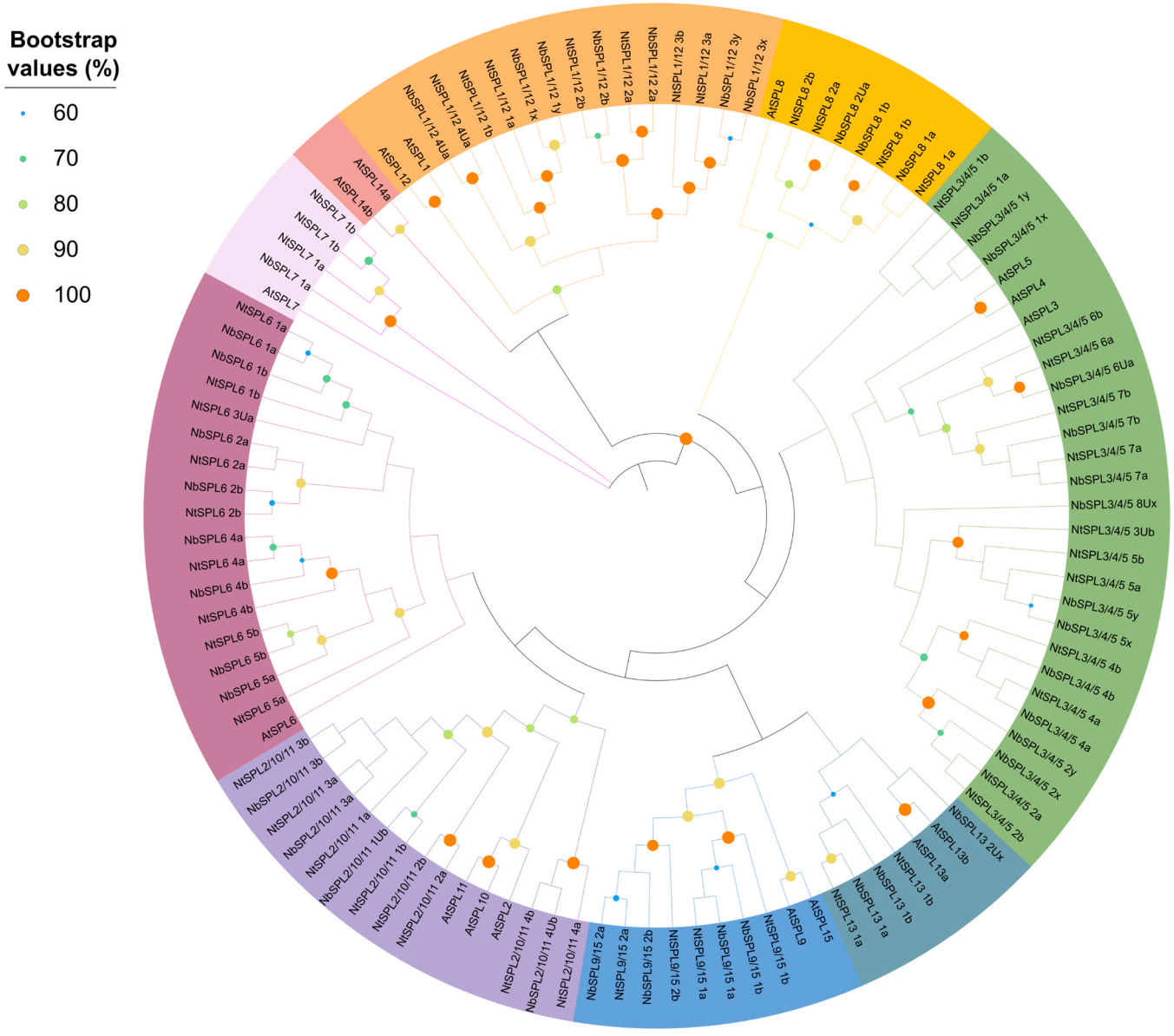

Fig. 1. Phylogenetic tree with *SPL* genes from *N. tabacum* cv. K326, *N. benthamiana* and *A. thaliana*. Phylogenetic tree was constructed from 16 *A. thaliana*, 49 *N. tabacum* cv. K326 and 43 *N. benthamiana* SPL proteins using the maximum-likelihood method with a bootstrap value of n = 1000 iterations. Bootstrap support values are represented in percentages.

3. Results

3.1. Phylogenetic analysis of the SPL family in N. tabacum and N. benthamiana

Putative SPL protein sequences from *N. tabacum* cv. K326 and *N. benthamiana* were retrieved as described in Materials and Methods. These sequences were aligned together with SPLs from *A. thaliana* and a phylogenetic tree was constructed using maximum likelihood method, with a bootstrap value of n = 1000 iterations (Fig. 1). All *SPL* genes were named as explained in Materials and Methods. In total, 49 *N. tabacum* cv. K326 and 43 *N. benthamiana* genes were identified and classified together with their *A. thaliana* homologues in eight differentiated clusters, namely *SPL1/12, SPL8, SPL13, SPL6, SPL7, SPL2/10/11, SPL9/15*, and *SPL3/4/5*. The different groups were named according to the *Arabidopsis SPL* gene appearing in the same clade. As it can be observed in the tree, all newly catalogued *Nicotiana* genes were distributed in one of the *Arabidopsis*-defined groups, but no *Nicotiana SPL* genes were found belonging to the *SPL14 Arabidopsis*-defined group. There was a markedly unequal distribution of the number of genes per clade. For example, the *SPL3/4/5* clade comprised 13 genes in *N. tabacum* cv. K326 and 12 in *N. benthamiana*, while the *SPL7* clade comprised only 2 genes in each species. Given the allotetraploid nature of both *Nicotiana* species, in most cases *SPL* genes were grouped in pairs of homeologous genes. When possible, we assigned each *SPL* of the same homeologous pair to the putative parental genome, which for *N. tabacum* cv. K326 are *N. sylvestris* and *N. tomentosiformis* (Sierro et al., 2014). Regarding *N. benthamiana*, performing this task was not so straightforward, due to the uncertainty about its origins. It was already hypothesized that *Noctiflorae* and *Sylvestres* sections were implicated in the genesis of *N. benthamiana* (Chase et al., 2003; Clarkson et al., 2004; Knapp et al., 2004), while a more recent study suggested that it could have originated from an introgression of *Petunioides* section into a member of *Noctiflorae* section that later hybridized with a member of *Sylvestres* section (Schiavinato et al., 2020). Given its complex origin, we did not have sufficient information to separate the subgenomes of *N. benthamiana*, and therefore we were not able to assign each *SPL* gene from the same homeologous pair to a specific parental genome. To facilitate their identification, the genes in the tree were given names that paired with their closest homeologs (e.g., 1a-1b, 2a-2b, 3x-3y, etc). Genes having the same number and letter for *N. benthamiana* and *N. tabacum* cv. K326 were homologous, allegedly coming from a common ancestor (for example *NtSPL7_1a* and *NbSPL7_1a*). In some cases, there were *SPL* genes that did not have an homeologous partner, probably due to loss during evolution. Therefore, they were named with a number followed by U, standing for "unique".

3.2. Protein structure of SPL genes: the SBP domain

The length and structure of the *N. benthamiana* and *N. tabacum* cv. K326 SPL proteins was analysed and shown in Table S2. Among all the clades, groups SPL3/4/5 and SPL13 were the ones with the smallest proteins. All *N. benthamiana* and *N. tabacum* cv. K326 SPLs in these groups had a range of amino acids from 100 to 200 except for NbSPL3/4/5_1y (395 aa), NtSPL3/4/5_1a (402 aa) and NtSPL3/4/5_1b (380 aa). The largest proteins were those in clade SPL1/12 with 900–1000 amino acids, being the only exception NbSPL1/12_4Ua with 362 amino acids.

To gain a better understanding of the SPL protein characteristics in *N. benthamiana* and *N. tabacum* cv. K326, their amino acid sequences were analysed using the MEME software to find conserved motifs along them (Fig. 2A, B). In total, ten conserved motifs were identified, but only members in the SPL1/12 group contained all ten motifs. Motifs 1, 2 and 3 represent together the SBP domain, which is close to the N-terminus and is key for the function of the SPL genes. Some proteins had a shorter SBP domain. This occurred in NtSPL13_1a, NtSPL3/4/5_5b, NtSPL6_5a, NtSPL8_2b, NbSPL2/10/11_1Ub and in the pair NbSPL3/4/5_5. Some proteins that were initially identified as SPLs using the whole sequence similarity criteria, turned out not to contain SBP domains, and were not included in Fig. 2. For *N. benthamiana*, these were NbSPL1/12_4Ua, NbSPL13_1b, NbSPL13_2Ux, NbSPL3/4/5_1x, NbSPL3/4/5_8Ux and NbSPL6_1a. In *N. tabacum* cv. K326, only protein NtSPL2/10/11_3b was missing the SBP domain. Only proteins of clades SPL1/12 and SPL7 had additional motifs to 1, 2 and 3. Seven extra motifs were present in the case of SPL1/12 and two in SPL7, most of them with unknown function.

Sequence alignment of the SBP domains of all NbSPLs and NtSPLs showed several highly conserved amino acids and a conserved structure (Fig. 2C). Fig. 2D shows the SBP domain of SPL9/15 from both species as an example. In this alignment the three motifs mentioned above can be clearly identified: the first Zinc-finger motif (Zn-1) Cys-Cys-Cys-His, the second one (Zn-2) Cys-Cys-His-Cys, and the nuclear localization signal (NLS).

3.3. Gene structure of SPL genes: exon-intron structure, putative miRNA156 target site

Nucleotide sequences of *SPL* genes were analysed for their exon-intron structure and for the presence of miR156 binding sites. As observed in Fig. 3, each clade had a well-defined exon-intron structure which was fairly conserved in all its members, but which differed strongly from other clades. Similarly, the presence/absence and the position of the putative target site for miR156 was a group-defining feature. Clades *SPL1/12*, *SPL7* and *SPL8* lacked miR156 target sites, while in the remaining clades most of their members contain a possible target position for miRNA156. The few exceptions to this general rule (e.g., *NbSPL2/10/11_1Ub, NtSPL6_5a* or *Nt_SPL3/4/5_5b*) were genes classified within a given clade but lacking the miRNA156 putative target site. These genes had also non-conserved exon-intron structures and were likely to be truncated genes or pseudogenes. Interestingly, both clade-specific gene structures and miRNA156 positions were strikingly well conserved between the two species, suggesting a strong selection and therefore a functional significance for both types of features. As expected, *N. tabacum* cv. K326 contained the same or more genes per clade than *N. benthamiana,* with the only exception of the *SPL13* clade, with three members in *N. benthamiana* and only two in *N. tabacum* cv. K326. However, as it can be observed also in Fig. 3 (left), only one of the representatives of the *NbSPL13* group had the expected exon-intron structure (and the SBP domain), whereas the remaining two had a smaller gene size and lacked a SBP domain, suggesting a possible ongoing process of pseudogenization for these two genes (*SPL13_1b* and *SPL13_Ux*).

3.4. Expression analysis of SPL genes in leaves

To determine the temporal expression patterns of *NbSPL* and *NtSPL* genes, we performed an RNA-seq analysis on *N. tabacum* cv. K326 and *N. benthamiana* leaf samples collected at three different growth stages. All RNA samples were isolated from the same leaf in different plants (leaf number five counting from the first true leaf that appears during development), but at different developmental stages, namely juvenile (J), pre-flowering (P), and flowering (F), the latter with first flower primordia already present (Fig. 4A and B). Comparisons of the expression of the same gene in the different developmental stages were done using the CPM-normalized log2-transformed expression data as depicted in Fig. 4C and D, while comparisons of the expression levels between genes were done with the FPKM-normalized log2-transformed expression data as depicted in Fig. S1.

In general, several similarities in the *SPL* expression patterns could be found between the two species (see Figs. 4C and 4D). For instance, *SPL1/12* and *SPL7* were expressed at high levels for both *N. benthamiana* and *N. tabacum* cv. K326 (Figs. 4C and D, Fig. S1 and Table S2). In particular, the *SPL1/12_2* pair showed the highest expression in both species and, surprisingly, their abundance increased with time despite

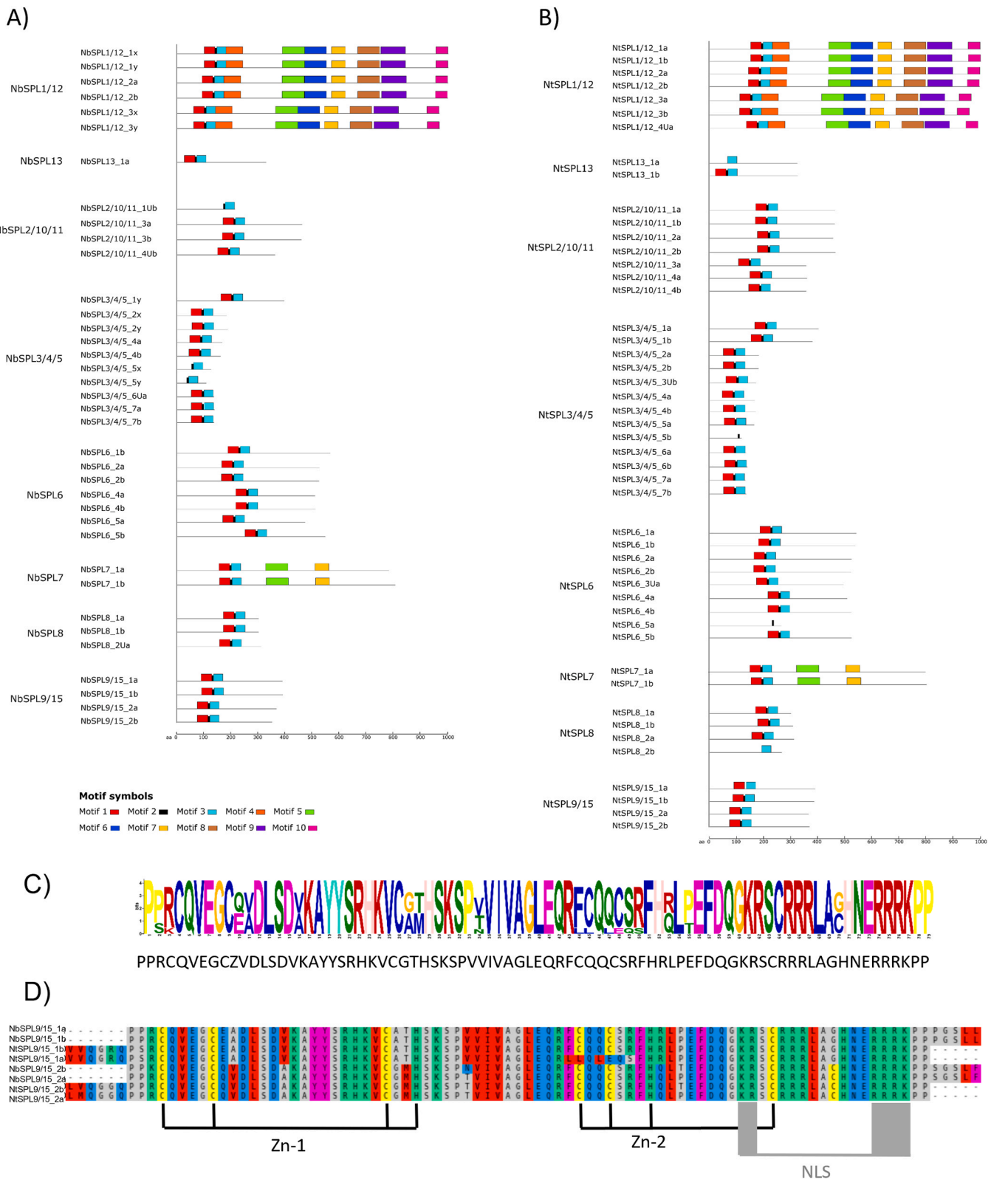

Fig. 2. Motifs composition and SBP domain of NbSPLs and NtSPLs. (A) Motifs along the NbSPL protein sequences, detected with MEME. Only *SPL* genes with SBP domain are shown. (B) Motifs along the NtSPL proteins sequences, detected with MEME. Only *SPL* genes with SBP domain are shown. (C) Motif logo and consensus sequence of the SBP domain of SPL9/15 proteins. Bits represent the conservation of sequence at a certain position. (D) Alignment of the SBP domains of *N. benthamiana* and *N. tabacum* cv. K326 SPL9/15 proteins. Multiple sequences alignment was performed using MAFFT version 7. The two Zn-finger like structures (Zn-1 and Zn-2) and the nuclear localization signal (NLS) are indicated.

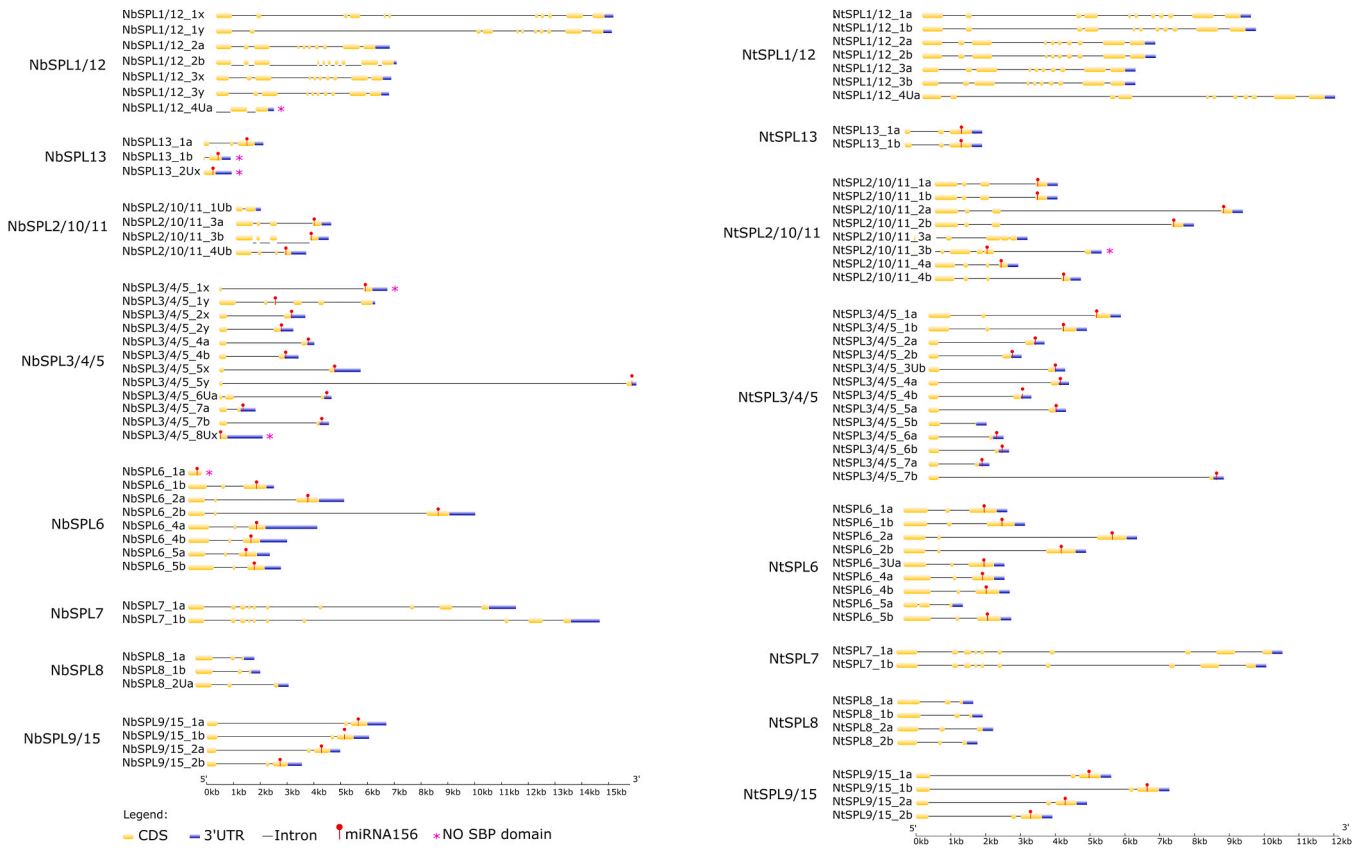

Fig. 3. Gene structure of NbSPLs (left) and NtSPLs (right). Exons, introns, CDS, 3' UTRs and miRNA156 annealing sites are shown. Genes with no SBP domain are indicated with a purple asterisk.

not being targets of miRNA156. Transcripts of *SPL1/12_1* and *SPL1/12_3* pairs were relatively less abundant but still detectable at high levels. As an exception, the *N. tabacum* cv. K326 gene *NtSPL1/12_4Ua* was expressed at very low levels in all stages. The second group by relative transcript abundance was *SPL7*. Both in *N. tabacum* cv. K326 and *N. benthamiana*, the two *SPL7* homeologues were highly expressed in all stages, although in *N. benthamiana* their expression was relatively lower. The high expression levels in all stages of these two clades could be partially explained by the fact that they were not repressed by miRNA156. However, this is not a general rule for all non-miRNA156 targets; *SPL8* genes were not regulated by miRNA156, but were poorly expressed in all stages for both species.

SPLs in groups under miRNA156 control were expressed at much lower levels, and this complicated the interpretation of the developmental fluctuations. In general, miRNA156 putative targets showed strong developmental variations in expression levels, although they did not necessarily follow the same trend in *N. tabacum* cv. K326 and *N. benthamiana*, something that could reflect different timings in developmental transitions between the two species. It was expected that miRNA156-regulated *SPLs* would increase their expression along the three developmental timepoints. This seemed to be the case for most genes in *N. benthamiana* (Fig. 4C), where this general trend could be observed in most members of *NbSPL3/4/5* and *NbSPL9/15* clades, and to a lesser extend also in the *NbSPL9/15* and *NbSPL6* clades, although not for *NbSPL2/10/11*. Interestingly, the strongest variation in the only canonical representative of the *NbSPL13* clade, the *NbSPL13_1a* gene, was observed for the transition between pre-flowering and flowering stages. In *N. tabacum* cv. K326, age-associated upregulation trends in miRNA156-regulated genes were less obvious, as we observed different behaviours in different members within the same clade (Fig. 4D). For instance, *NtSPL2/10/11_1a* and *NtSPL2/10/11_1b* were clearly downregulated as the leaves aged, whereas the other two representatives of the same clade showed constant expression levels. Similarly, *NtSPL6_3Ua* levels increased dramatically with age, whereas clade partners *NtSPL6_1a* and *NtSPL6_1b* followed the opposite trend. Interestingly, and contrary to what was observed in *N. benthamiana*, expression of the *NtSPL13* clade peaked at pre-flowering stage and was reduced drastically at flowering.

3.5. Gene editing of NbSPL13 gene subfamily resulted in delayed flowering

SPL genes are involved in various physiological processes whose manipulation could be advantageous for plant biofactories, like the extension of the pre-flowering phase. To obtain a first indication of the phenotypic effects that mutagenesis in the SPL family could have, we decided to knock out the *NbSPL13_1a* gene in *N. benthamiana*. *NbSPL13_1a* expression profile showed strong upregulation in the transition from pre-flowering to flowering stages, suggesting a role of this gene in flowering regulation. Furthermore, *NbSPL13* resulted as the smallest functional family in *N. benthamiana,* thus facilitating knock out strategy. As described earlier, among the three putative *NbSPL13* members, only *NbSPL13_1a* was likely to contribute to phase transition as it was the only one containing all canonical elements, namely an SPB domain and a miRNA156 putative target site. *NbSPL13_1b* had no SPB domain, whereas *NbSPL13_2Ux* was considered a pseudogene as there were no RNA reads associated to this gene. Two guide RNAs (gRNAs) were designed for targeting *NbSPL13_1a*: the sgSPL1.5 gRNA targeting exon 1 and the sgSPL1.6 gRNA for exon 2 (Table S1, Fig. 5A). Although both gRNAs targeted also *NbSPL13_1b* at exons 1 and 2, they were unlikely to produce an effect since according to the latest annotation of this gene they fall outside the predicted CDS.

A CRISPR/Cas9 construct was assembled that includes the nptII, Cas9 and DsRed TUs together with the gRNA TU (GB3298, Fig. 5B). The

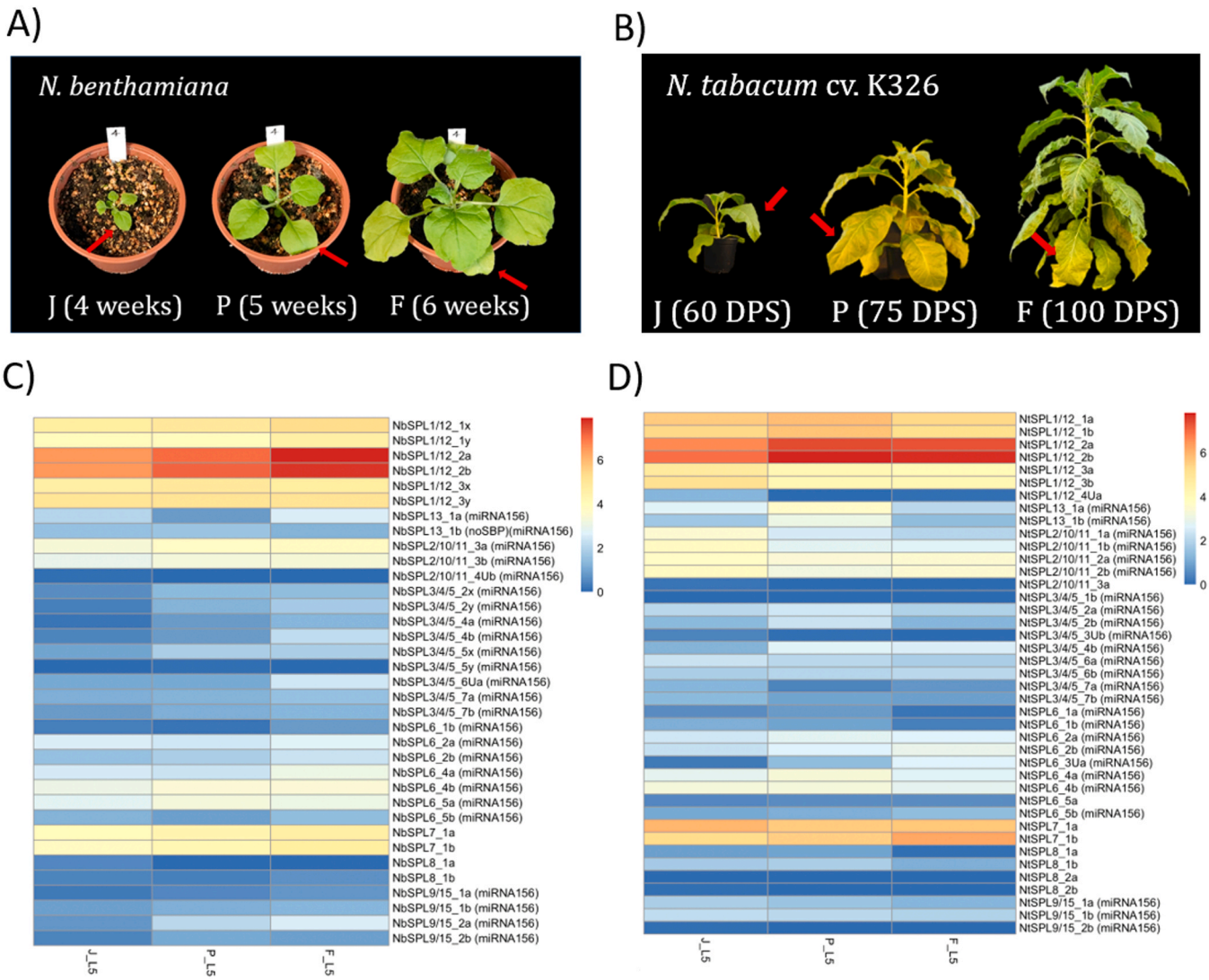

Fig. 4. Expression profiles of *NbSPL* and *NtSPL* genes in leaf at different developmental stages. Pictures of *N. benthamiana* (A) and *N. tabacum* cv. K326 (B) plants at juvenile (J), pre-flowering (P) and flowering (F) stages. Red arrows indicate the fifth true leaf. **C)** CPM-normalized log2-transformed expression values for *NbSPL* genes, based on transcriptome data. Each rectangle represents the mean of 3 replicates **D)** CPM-normalized log2-transformed expression values for *NtSPL* genes, based on transcriptome data. Each rectangle represents the mean of 3 replicates.

two gRNAs were expressed from a single U6–26 promoter using the tRNA strategy (Xie et al., 2015). This construct was used to transform a WT *N. benthamiana* plant, and eight primary transformants were obtained. All of them carried mutations at the sgSPL1.5-targeted site. Fig. 5C shows the percentage of mutations observed in the T0 generation for the sgSPL1.6-targeted site. One out of the eight regenerated plants was not edited, three of them were considered chimeras (percent editing reported by Synthego below 40%), three of them carried heterozygous mutations (percent editing reported by Synthego around 50%) and only one plant showed biallelic mutations in *NbSPL13_1a* (>90%). The plant with biallelic mutations in *NbSPL13_1a* (nr. 3) carried a four-nucleotides deletion at the targeted site, but also contained a heterozygous mutation in *NbSPL13_1b*. The T1 offspring of this plant was grown in a growth chamber together with WT plants and all of them were phenotyped by scoring the flowering time and the number of lateral branches at two different time points. To account for any unexpected effect of *NbSPL13_1b* mutations, each T1 plant in the analysis was genotyped for *NbSPL13_1b*. In total 4 groups of plants were analysed: WT, *NbSPL13_1a/1a* (biallelic mutation in *NbSPL13_1a* and not edited in *NbSPL13_1b*), *NbSPL13_1a/1a/1b* (biallelic mutation in *NbSPL13_1a* and heterozygous mutation for *NbSPL13_1b*), *NbSPL13_1a/1a/1b/1b* (biallelic mutation for both homeologous genes).

The analysis of *NbSPL13* mutated lines clearly indicated a role of *NbSPL13_1a* in the control of flowering time. Plants of all mutant lines flowered almost simultaneously, showing an average delay of 4.5 days compared to WT (Fig. 6A). As expected, the status of *NbSPL13_1b* gene, whereas mutated in biallelic or heterozygous form, had no effect in the flowering time. As mentioned before, the gRNAs targeting this gene were unlikely to produce loss-of-function mutants since they targeted the 5'UTR sequence but not the CDS. The number of lateral branches at WT flowering time (38.25 ± 0.87 dps) was also recorded, at that time no significant differences were observed between mutant and WT plants (Fig. 6B). However, when branching was recorded for each plant at their respective flowering times, significant differences were observed between WT and mutant plants, with six branches on average for WT and ten on average for *SPL13_1a* knock-out lines (Fig. 6C). To discard that *NbSPL13* mutations could affect negatively recombinant protein production capacity, syringe-Agroinfiltration assays were performed using two different expression systems, namely a geminivirus and a TMV-based vector (see Materials and Methods). No significant differences in eGFP fluorescence were observed between mutant and WT lines (see Fig. S3).

A)

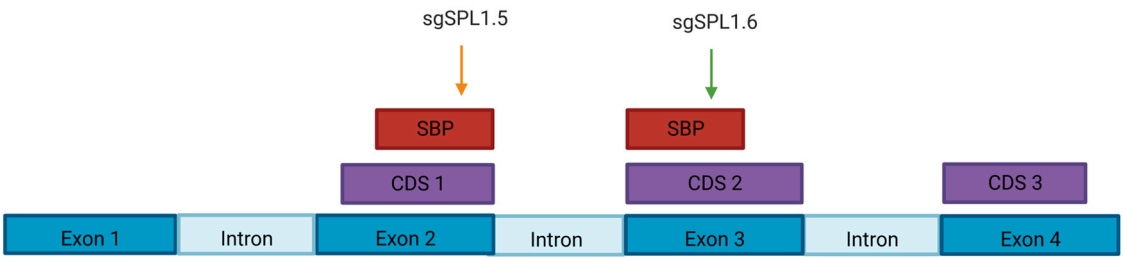

B)

C)

T0 plant	sgSPL1.6 % efficency	Predominant genomic sequence	Mutation
SPL13 1A	48	CAGGCGTTCGAAGGAAA	T insertion in heterozygosis
SPL13 3	92	CAG/CGAAGGAAA	-4 deletion (biallelic)
SPL13 6	19	CAGGCGTCGAAGGAAA	Chimera
SPL13 7	0	CAGGCGTCGAAGGAAA	WT
SPL13 8	53	CAGGCGTTCGAAGGAAA	T insertion in heterozygosis
SPL13 9	34	CAGGCGTCGAAGGAAA	Chimera
SPL13 10	15	CAGGCGTCGAAGGAAA	Chimera
SPL13 11	48	CAGGCGTTCGAAGGAAA	T insertion in heterozygosis

Fig. 5. Generation of *N. benthamiana* lines edited in *NbSPL13_1a* gene. A) Structure of *NbSPL13_1a*, exons are indicated in blue, introns in light blue, CDSs in violet, and SBP domain in red. Arrows represent sgRNAs sgSPL1.5 and sgSPL1.6. B) Vector GB3298 used for transformation to edit *NbSPL13* genes. Violet arrows: promoters of nptII, Cas9 and DsRed. Orange Ts: terminators. The green arrow represents U6–26 promoter, followed by TU constituted by guides sgSPL1.5, sgSPL1.6. C) Table representing the T0 obtained from the transformation. For each plant are reported the editing efficiency values of sgSPL1.6 guide reported by Synthego, its predominant genomic sequence at the cut site, and the corresponding mutation. Letters highlighted in red represent base insertions. Plant 3 is highlighted, since it was the one selected for following with T1 generation.

4. Discussion

SPLs are plant-specific transcription factors that play an important role in many aspects of plant development, including branching, leaf initiation rate or flowering time (Ferreira e Silva et al., 2014; Preston and Hileman, 2013; H. Wang and Wang, 2015; Xu et al., 2016; Yu et al., 2015). Many of them are subjected to miRNA156 control, whose expression level decreases throughout plant growth, allowing to express *SPL* genes in later stages of plant development (H. Wang and Wang, 2015; Xu et al., 2016; T. Zhang et al., 2015). Therefore, the miR156/SPL module has been proposed as a toolset for crop improvement (H. Wang and Wang, 2015; T. Zhang et al., 2015), as SPL genes are relevant targets for improving agronomic traits such as ideal plant architecture, better yield and optimal flowering time (H. Wang and Wang, 2015; T. Zhang et al., 2015). *Nicotiana* plants are routinely used at lab scale for added-value compounds manufacturing. Despite their several advantages, including their non-food status, fast growth, or amenability for genetic transformation and Agroinfiltration, they are not yet optimal biofactories (Alkanaimsh et al., 2019). Breeding objectives for Nicotiana towards this aim include biomass increase, delay in flowering time or more lateral branching, associated to higher yield upon Agroinfiltration (Goulet et al., 2019). Thus, manipulating *SPL* genes may represent a reasonable approach for breeding *Nicotiana* as improved biofactories.

In this work, we performed a genome-wide analysis of *SPL* genes in the two more relevant *Nicotiana* species for biofactory use, namely *N. benthamiana* and *N. tabacum* cv. K326 (Bally et al., 2018; Ma et al., 2015; Molina-Hidalgo et al., 2021; van Herpen et al., 2010). Phylogenetic tree analysis showed that *NbSPLs* and *NtSPLs* clustered into eight groups, observing a similar number of *N. benthamiana* and *N. tabacum* cv. K326 genes within each group: seven *SPL1/12* genes, three *SPL13* genes for *N. benthamiana* and two for *N. tabacum* cv. K326, four *SPL2/10/11* genes for *N. benthamiana* and eight for *N. tabacum* cv. K326,

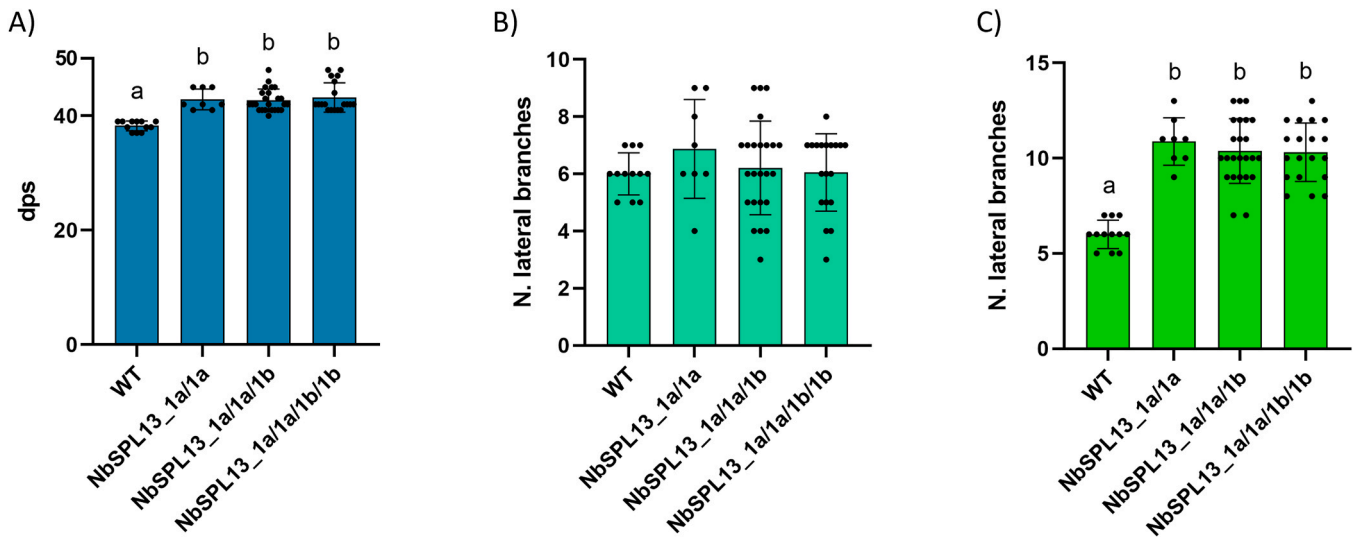

Fig. 6. Phenotype of *NbSPL13* edited lines. Phenotyping parameters of the plants grown in growth chamber. To account for any unexpected effect of *NbSPL13_1b* mutations, each T1 plant in the analysis was genotyped for *NbSPL13_1b*. In total 4 groups of plants were analysed: WT, *NbSPL13_1a/1a* (biallelic mutation in *NbSPL13_1a* and not edited in *NbSPL13_1b*), *NbSPL13_1a/1a/1b* (biallelic mutation in *NbSPL13_1a* and heterozygous mutation for *NbSPL13_1b*), *NbSPL13_1a/1a/1b/1b* (biallelic mutation for both homeologous genes). A) Flowering time expressed as days post sowing (dps). B) Number of lateral branches at flowering time of the WT plants. C) Number of lateral branches at flowering time of each plant. Each bar represents mean value ± SD (n = 12 for WT, n = 8 for *NbSPL13_1a/1a*, n = 22 for *NbSPL13_1a/1a/1b* and n = 19 for *NbSPL13_1a/1a/1b/1b*). A one-way ANOVA test was performed ($p < 0.05$). Groups marked with the same letter have no significant differences among them, if marked with different letters they differ significantly.

12 *SPL3/4/5* genes for *N. benthamiana* and 13 for *N. tabacum* cv. K326, eight *SPL6* genes for *N. benthamiana* and nine for *N. tabacum* cv. K326, two *SPL7* genes for both, three *SPL8* genes for *N. benthamiana* and four for *N. tabacum* cv. K326, and four *SPL9/15* genes for both. Only for group *SPL2/10/11* there was a difference greater than one between the number of proteins for both species, with eight *NtSPLs* while only four *NbSPLs*. The lower total number of SPL genes in *N. benthamiana* as compared to *N. tabacum* cv. K326 was to be expected as the result of the diploidization process, provided that the earlier is an ancient allotetraploid, whereas tetraploidization was a relatively recent phenomenon in the latter (Edwards et al., 2017; Schiavinato et al., 2020; Sierro et al., 2014).

The new version of the *N. benthamiana* genome (https://www.nbenth.com/) (*Nicotiana benthamiana Genome & Wild Transcriptome Site*, n.d.; Ranawaka et al., 2022) and the Edwards v4.5 version of the *N. tabacum* cv. K326 genome (Edwards et al., 2017) facilitated the genome-wide identification of the *NbSPLs* and *NtSPLs*. Gene models were confirmed with our own RNAseq data for most *SPLs*. However, the transcript levels of some genes were below detection levels, and further research is needed to validate the structural annotation of those genes. We identified several conserved motifs in the SPL family members for both species. While the purpose of most motifs remained unknown, the three motifs that consistently appeared in all potentially functional SPLs were the ones comprising the SBP domain. This domain is crucial for their binding to DNA and consequently for their role as transcription factors (Xu et al., 2016). We identified in the SBP domain of NbSPLs and NtSPLs two zinc finger motifs and one nuclear localisation signal, as it occurs in SPL proteins of other species (Cai et al., 2018; Cardon et al., 1999; Li & Lu, 2014; Liu et al., 2019; Mao et al., 2016; Pan et al., 2017; Salinas et al., 2012; Song et al., 2016; Tripathi et al., 2018; Z. Yang et al., 2008; Zeng et al., 2019; Zhou et al., 2018). Six of the *N. benthamiana* and one of the *N. tabacum* cv. K326 proteins initially identified as SPLs in our search, did not contain a SBP domain and therefore it is unlikely that they can function as transcription factors. On the other hand, it is very likely that those genes classified in the same clade play similar biological functions, given the high sequence homology among them, their similar gene structure, and the presence of the same conserved motifs.

As an additional step towards the functional characterization of the *SPL* family in Nicotiana genus, we performed a transcriptomic analysis of equivalent leaves at three developmental time points: juvenile, pre-flowering and early post-flowering. Some of the analyzed genes showed undetectable expression levels. For example, transcripts were not detected in those genes lacking the SBP domain with exception of *NbSPL13_1b*. The remaining genes were expressed in all developmental stages at different levels. Some genes not under miRNA156 control, such as those in groups *SPL1/12* and *SPL7*, were broadly expressed at high levels in both species. However, this is not true for *SPL8* - it was not regulated by miRNA 156, but had lower expression. A similar behaviour can be observed also in other species. *SPL1*, *SPL12* and *SPL7* exhibit a high expression in leaves of *A. thaliana* (Moreno et al., 2022) and cotton (Cai et al., 2018). In leaves of chrysanthemum *SPL1* and *SPL7* are highly expressed, while *SPL12* is expressed at low levels (Song et al., 2016). Regarding *SPL8*, it shows a very low level of expression in *A. thaliana* (Moreno et al., 2022) and cotton (Cai et al., 2018), while in chrysanthemum, on the contrary, is highly expressed (Song et al., 2016).

In *N. benthamiana* and *N. tabacum* cv. K326, unexpectedly, not all groups of miRNA156-regulated *SPLs* showed a progressive increase in expression with plant age. In general, they were all expressed at much lower levels compared to *SPL1/12* and *SPL7*. Some groups globally exhibited a progressively increasing expression as expected, whereas others showed different behaviours. This was true also for *SPL13* subfamily in *N. benthamiana*: *NbSPL13_1a* decreased from juvenile to pre-flowering stage, but then increased at flowering. Its partner *NbSPL13_1b* with no SBP domain stayed at similar expression level from juvenile to pre-flowering stage and decreased at flowering. The low level of expression for most of *SPL* genes could be explained by the fact that all SPL proteins belonging to the same group have redundant functions, so that the expression of a single *SPL* gene is not required to be high. The unexpected behaviour of various *SPL* genes regulated by miR156 could be due to a complex transcriptional behaviour occurring in this large family, which may include tissue-specific regulation or complex time fluctuations that could have escaped from the general experimental setup followed here. A more detailed expression profile analysis for each gene family should follow to provide a more complete picture of the entire *SPL* regulatory complex in these two species.

Following the structural characterization and the gene expression

analysis of the *NbSPL* genes, we wanted to explore the potential of SPLs as targets for breeding new biofactory-oriented traits. Particularly, we decided to study whether the knock-out of the smallest functional SPL group in *N. benthamiana*, *NbSPL13*, had an influence on the plant architecture and flowering time.

Previous studies have conducted loss-of-function experiments targeting *SPL* genes in different species, revealing various phenotypic effects. In rice, CRISPR/Cas-mediated knockout of individual *SPL* genes resulted in defects in plant height, reduced panicle size and altered grain length (Jiang et al., 2020). In barley, loss of *HvSPL8* function confers smaller leaves angle: this feature allows lower leaves to be shed by more light, increasing photosynthesis rate and therefore productivity (S. Yang et al., 2022). In *N. tabacum* cv. K326 the overexpression of miRNA156, with the subsequent down-regulation of the miR156-targeted *SPL* genes, resulted in delayed flowering and a higher leaves production rate (Feng et al., 2016) and the generation of biallelic mutations in 9 *SPL* genes with CRISPR/Cas caused delayed flowering, leaf juvenility and more branching (Vazquez-Vilar et al., 2021). On the other hand, gain of function mutations in *OsSPL14* in rice confers an ideal plant architecture with thick culm, large panicle and reduced tillers (Jiao et al., 2010; J. Wang et al., 2017).

Regarding *SPL13*, previous studies in alfalfa showed that this gene has an important role in drought stress tolerance (Arshad et al., 2017; Feyissa et al., 2019) and vegetative-floral transition. Gao at al. demonstrated in 2018 that *SPL13* silencing caused a delay in flowering time and increased number of lateral branches in this species (Gao et al., 2018). Using CRISPR/Cas9, we obtained a plant carrying a biallelic deletion of 4 nucleotides in the first exon of *NbSPL13_1a* and a heterozygous mutation in the 5'UTR of *NbSPL13_1b*. The progeny of this plant was phenotyped for flowering time and all T1 plants exhibited a significant delay in flowering of 4–5 days with respect to WT.

It is a common practice both in academic and industrial experimental setups, to perform Agroinfiltration before the plants reach the flowering stage, as it is well known that expression levels drop dramatically afterwards (Sheludko et al., 2007). In this regard, plant varieties with delayed flowering time could give time to accumulate more productive biomass in the same growing area. Interestingly, we observed that late flowering was accompanied by an increase in the total number of lateral branches. Interestingly, Goulet et al. (2019) previously reported that young leaves in axillary stems are the main contributors to recombinant protein yield upon Agroinfiltration (Goulet et al., 2019). Therefore, we anticipate that the combination late flowering and increased branching in *NbSPL13_1a* KO phenotype should lead to gains in recombinant protein yield per batch. However, as with field trials in traditional breeding of food crops, the full advantage conferred by this new trait to the *N. benthamiana* biofactory can only be confirmed in a real-life scenario, which in this case implies a pilot vacuum infiltration experiment in an industrial setup. Syringe-infiltration experiments showed no differences in expression in *NbSPL13* KO compared to WT. However, these experiments do not appraise the potential advantages of the mutants, that would need to be assessed at a larger scale. Furthermore, pilot experiments should be followed by a techno economical evaluation that integrate not only calculations of yield per batch, but also the number of batches per time unit, since yield gains per batch need to compensate the longer growing times associated with late flowering.

In our view this work shows how genomic insights in large gene families can inform and orient breeding strategies, especially in polypoid crops. It also illustrates how the breeding of plant biofactories can benefit from new precision techniques and vice versa, since this type of industrial crops, usually grown under contained conditions, offer minimal ethical, legal and/or environmental restrictions for commercial implementation even in the most restrictive economic zones as the EU.

5. Conclusions

Our work aimed at the identification of Squamosa Promoter Binding-Like (SPL) genes in *N. tabacum* cv. K326 and *N. benthamiana*. Fourty-nine *SPL* genes were found in *N. tabacum* cv. K326 and 43 in *N. benthamiana* LAB strain, and classified into eight phylogenetic groups according to the SPL classification in *Arabidopsis*. Homeologues and orthologues showed a conserved exon-intron gene structure and a conserved DNA-binding domain. Thirty of the *NbSPL* genes and 33 of the *NtSPL* genes were found to be putative targets of microRNA 156. Their expression in leaves was analysed by RNA-seq at three different stages, revealing that genes not under miR156 control were in general constitutively expressed at high levels, while miR156-regulated genes showed lower expression levels, often developmentally regulated. We chose to edit *NbSPL13_1a*, whose knock-out led to a delay in flowering time, a trait that could be exploited to increase biomass for recombinant protein production. In our view this work showed how genomic insights in large gene families can inform and orient breeding strategies, especially in polypoid crops.

Ethics approval and consent to participate

This study complies with institutional biosafety and biocontainment guidelines. This article does not contain any studies with human participants or animals performed by any of the authors.

Funding

This work was supported by grant H2020–760331 Newcotiana from the European Commission. C.D and M.V.V are the recipients of fellowships GRISOLIAP/2019/013 and APOSTD/2020/096 from the Generalitat Valenciana (Spain), respectively.

CRediT authorship contribution statement

Carmine De Paola, Marta Vazquez-Vilar: Experiments and data collection. **Victor Garcia-Carpintero, Kacper Kaminski**: Bioinformatical analyses. **Diego Orzaez, Asun Fernandez-del-Carmen**: Funding acquisition, Supervision. **Carmine De Paola**: Writing – original draft. **Marta Vazquez-Vilar, Victor Garcia-Carpintero, Diego Orzaez, Giovanni Giuliano, Nicolas Sierro, Nikolai V. Ivanov, Kacper Kaminski, Peter Waterhouse**: Writing – review & editing.

Declaration of Competing Interest

The authors declare that they have no known competing financial interests or personal relationships that could have appeared to influence the work reported in this paper.

Data availability

Data will be made available on request.

Appendix A. Supporting information

Supplementary data associated with this article can be found in the online version at doi:10.1016/j.plantsci.2023.111797.

References

S. Alkanaimsh, J.M. Corbin, M.J. Kailemia, K. Karuppanan, R.L. Rodriguez, C.B. Lebrilla, K.A. McDonald, S. Nandi, Purification and site-specific N-glycosylation analysis of human recombinant butyrylcholinesterase from Nicotiana benthamiana, Biochem. Eng. J. 142 (2019) 58–67, https://doi.org/10.1016/j.bej.2018.11.004.

S.F. Altschul, W. Gish, W. Miller, E.W. Myers, D.J. Lipman, Basic local alignment search tool, J. Mol. Biol. 215 (3) (1990) 403–410, https://doi.org/10.1016/S0022-2836(05)80360-2.

M. Arshad, B.A. Feyissa, L. Amyot, B. Aung, A. Hannoufa, MicroRNA156 improves drought stress tolerance in alfalfa (Medicago sativa) by silencing SPL13, Plant Sci. 258 (2017) 122–136, https://doi.org/10.1016/j.plantsci.2017.01.018.

J. Bally, H. Jung, C. Mortimer, F. Naim, J.G. Philips, R. Hellens, A. Bombarely, M. M. Goodin, P.M. Waterhouse, The Rise and Rise of Nicotiana benthamiana: A Plant for All Reasons, Annu. Rev. Phytopathol. 56 (2018) 405–426, https://doi.org/10.1146/annurev-phyto-080417-050141.

R.P. Birkenbihl, G. Jach, H. Saedler, P. Huijser, Functional dissection of the plant-specific SBP-domain: Overlap of the DNA-binding and nuclear localization domains, J. Mol. Biol. 352 (3) (2005) 585–596, https://doi.org/10.1016/j.jmb.2005.07.013.

A.M. Bolger, M. Lohse, B. Usadel, Trimmomatic: A flexible trimmer for Illumina sequence data, Bioinforma. (Oxf., Engl.) 30 (15) (2014) 2114–2120, https://doi.org/10.1093/bioinformatics/btu170.

C. Cai, W. Guo, B. Zhang, Genome-wide identification and characterization of SPL transcription factor family and their evolution and expression profiling analysis in cotton, Sci. Rep. 8 (1) (2018) 762, https://doi.org/10.1038/s41598-017-18673-4.

G. Cardon, S. Höhmann, J. Klein, K. Nettesheim, H. Saedler, P. Huijser, Molecular characterisation of the Arabidopsis SBP-box genes, Gene 237 (1) (1999) 91–104, https://doi.org/10.1016/s0378-1119(99)00308-x.

M.W. Chase, S. Knapp, A.V. Cox, J.J. Clarkson, Y. Butsko, J. Joseph, V. Savolainen, A. S. Parokonny, Molecular systematics, GISH and the origin of hybrid taxa in Nicotiana (Solanaceae, Ann. Bot. 92 (1) (2003) 107–127, https://doi.org/10.1093/aob/mcg087.

J.J. Clarkson, S. Knapp, V.F. Garcia, R.G. Olmstead, A.R. Leitch, M.W. Chase, Phylogenetic relationships in Nicotiana (Solanaceae) inferred from multiple plastid DNA regions, Mol. Phylogenet. Evol. 33 (1) (2004) 75–90, https://doi.org/10.1016/j.ympev.2004.05.002.

T. Dahan-Meir, S. Filler-Hayut, C. Melamed-Bessudo, S. Bocobza, H. Czosnek, A. Aharoni, A.A. Levy, Efficient in planta gene targeting in tomato using geminiviral replicons and the CRISPR/Cas9 system, Plant J. 95 (1) (2018) 5–16, https://doi.org/10.1111/tpj.13932.

X. Dai, Z. Zhuang, P.X. Zhao, psRNATarget: A plant small RNA target analysis server (2017 release, Nucleic Acids Res. 46 (W1) (2018) W49–W54, https://doi.org/10.1093/nar/gky316.

B. Diego-Martin, B. González, M. Vazquez-Vilar, S. Selma, R. Mateos-Fernández, S. Gianoglio, A. Fernández-del-Carmen, D. Orzáez, Pilot Production of SARS-CoV-2 Related Proteins in Plants: A Proof of Concept for Rapid Repurposing of Indoor Farms Into Biomanufacturing Facilities, *Front. Plant Sci.* 11 (2020), https://doi.org/10.3389/fpls.2020.612781.

L. Derevnina, S. Kamoun, C.-H. Wu, Dude, where is my mutant? Nicotiana benthamiana meets forward genetics, The New Phytologist 221 (2) (2019) 607–610, https://doi.org/10.1111/nph.15521.

R.C. Edgar, MUSCLE: Multiple sequence alignment with high accuracy and high throughput, Nucleic Acids Res. 32 (5) (2004) 1792–1797, https://doi.org/10.1093/nar/gkh340.

K.D. Edwards, N. Fernandez-Pozo, K. Drake-Stowe, M. Humphry, A.D. Evans, A. Bombarely, F. Allen, R. Hurst, B. White, S.P. Kernodle, J.R. Bromley, J.P. Sanchez-Tamburrino, R.S. Lewis, L.A. Mueller, A reference genome for Nicotiana tabacum enables map-based cloning of homeologous loci implicated in nitrogen utilization efficiency, BMC Genom. 18 (1) (2017) 448, https://doi.org/10.1186/s12864-017-3791-6.

S. Feng, Y. Xu, C. Guo, J. Zheng, B. Zhou, Y. Zhang, Y. Ding, L. Zhang, Z. Zhu, H. Wang, G. Wu, Modulation of miR156 to identify traits associated with vegetative phase change in tobacco (Nicotiana tabacum), J. Exp. Bot. 67 (5) (2016) 1493–1504, https://doi.org/10.1093/jxb/erv551.

G.F. Ferreira e Silva, E.M. Silva, M. Azevedo, S. da, M.A.C. Guivin, D.A. Ramiro, C. R. Figueiredo, H. Carrer, L.E.P. Peres, F.T.S. Nogueira, MicroRNA156-targeted SPL/SBP box transcription factors regulate tomato ovary and fruit development, Plant J.: Cell Mol. Biol. 78 (4) (2014) 604–618, https://doi.org/10.1111/tpj.12493.

B.A. Feyissa, M. Arshad, M.Y. Gruber, S.E. Kohalmi, A. Hannoufa, The interplay between miR156/SPL13 and DFR/WD40-1 regulate drought tolerance in alfalfa, BMC Plant Biol. 19 (1) (2019) 434, https://doi.org/10.1186/s12870-019-2059-5.

M. Gandikota, R.P. Birkenbihl, S. Höhmann, G.H. Cardon, H. Saedler, P. Huijser, The miRNA156/157 recognition element in the 3' UTR of the Arabidopsis SBP box gene SPL3 prevents early flowering by translational inhibition in seedlings, Plant J.: Cell Mol. Biol. 49 (4) (2007) 683–693, https://doi.org/10.1111/j.1365-313X.2006.02983.x.

R. Gao, M.Y. Gruber, L. Amyot, A. Hannoufa, SPL13 regulates shoot branching and flowering time in Medicago sativa, Plant Mol. Biol. 96 (1–2) (2018) 119–133, https://doi.org/10.1007/s11103-017-0683-8.

H. Gielen, T. Remans, J. Vangronsveld, A. Cuypers, Toxicity responses of Cu and Cd: The involvement of miRNAs and the transcription factor SPL7, BMC Plant Biol. 16 (1) (2016) 145, https://doi.org/10.1186/s12870-016-0830-4.

Giritch, A., Marillonnet, S., Engler, C., van Eldik, G., Botterman, J., Klimyuk, V., & Gleba, Y. (2006). Rapid high-yield expression of full-size IgG antibodies in plants coinfected with noncompeting viral vectors. Proceedings of the National Academy of Sciences, 103(40), 14701–14706. https://doi.org/10.1073/pnas.0606631103.

M.M. Goodin, D. Zaitlin, R.A. Naidu, S.A. Lommel, Nicotiana benthamiana: Its history and future as a model for plant-pathogen interactions, Molecular Plant-Microbe Interactions: MPMI 21 (8) (2008) 1015–1026, https://doi.org/10.1094/MPMI-21-8-1015.

M.-C. Goulet, L. Gaudreau, M. Gagné, A.-M. Maltais, A.-C. Laliberté, G. Éthier, N. Bechtold, M. Martel, M.-A. D'Aoust, A. Gosselin, S. Pepin, D. Michaud, Production of Biopharmaceuticals in Nicotiana benthamiana—Axillary Stem Growth as a Key Determinant of Total Protein Yield, *Front. Plant Sci.* 10 (2019), https://doi.org/10.3389/fpls.2019.00735.

Y.-Y. Han, Y.-Q. Ma, D.-Z. Li, J.-W. Yao, Z.-Q. Xu, Characterization and phylogenetic analysis of fifteen NtabSPL genes in Nicotiana tabacum L. cv. Qinyan95, Dev. Genes Evol. 226 (1) (2016) 1–14, https://doi.org/10.1007/s00427-015-0522-3.

R.B. Horsch, J.E. Fry, N.L. Hoffmann, M. Wallroth, D. Eichholtz, S.G. Rogers, R.T. Fraley, A Simple and General Method for Transferring Genes into Plants, Science 227 (4691) (1985) 1229–1231, https://doi.org/10.1126/science.227.4691.1229.

M. Jiang, Y. He, X. Chen, X. Zhang, Y. Guo, S. Yang, J. Huang, M.B. Traw, CRISPR-based assessment of genomic structure in the conserved SQUAMOSA promoter-binding-like gene clusters in rice, Plant J. 104 (5) (2020) 1301–1314, https://doi.org/10.1111/tpj.15001.

Y. Jiao, Y. Wang, D. Xue, J. Wang, M. Yan, G. Liu, G. Dong, D. Zeng, Z. Lu, X. Zhu, Q. Qian, J. Li, Regulation of OsSPL14 by OsmiR156 defines ideal plant architecture in rice, Nat. Genet. 42 (6) (2010) 541–544, https://doi.org/10.1038/ng.591.

K. Katoh, J. Rozewicki, K.D. Yamada, MAFFT online service: Multiple sequence alignment, interactive sequence choice and visualization, Brief. Bioinforma. 20 (4) (2019) 1160–1166, https://doi.org/10.1093/bib/bbx108.

D. Kim, J.M. Paggi, C. Park, C. Bennett, S.L. Salzberg, Graph-based genome alignment and genotyping with HISAT2 and HISAT-genotype, Nature Biotechnology 37 (8) (2019) 907–915, https://doi.org/10.1038/s41587-019-0201-4.

J. Klein, H. Saedler, P. Huijser, A new family of DNA binding proteins includes putative transcriptional regulators of the Antirrhinum majus floral meristem identity gene SQUAMOSA, Mol. Gen. Genet.: MGG 250 (1) (1996) 7–16, https://doi.org/10.1007/BF02191820.

S. Knapp, L. Bohs, M. Nee, D.M. Spooner, Solanaceae—A model for linking genomics with biodiversity, Comp. Funct. Genom. 5 (3) (2004) 285–291, https://doi.org/10.1002/cfg.393.

C. Li, S. Lu, Molecular characterization of the SPL gene family in Populus trichocarpa, BMC Plant Biol. 14 (2014) 131, https://doi.org/10.1186/1471-2229-14-131.

M. Liu, W. Sun, Z. Ma, L. Huang, Q. Wu, Z. Tang, T. Bu, C. Li, H. Chen, Genome-wide identification of the SPL gene family in Tartary Buckwheat (Fagopyrum tataricum) and expression analysis during fruit development stages, BMC Plant Biol. 19 (1) (2019) 299, https://doi.org/10.1186/s12870-019-1916-6.

Ma, J.K.-C., Drossard, J., Lewis, D., Altmann, F., Boyle, J., Christou, P., Cole, T., Dale, P., van Dolleweerd, C.J., Isitt, V., Katinger, D., Lobedan, M., Mertens, H., Paul, M.J., Rademacher, T., Sack, M., Hundleby, P.A.C., Stiegler, G., Stoger, E., … Fischer, R.. (2015). Regulatory approval and a first-in-human phase I clinical trial of a monoclonal antibody produced in transgenic tobacco plants. *Plant Biotechnology Journal*, *13*(8), 1106–1120. https://doi.org/10.1111/pbi.12416.

H.-D. Mao, L.-J. Yu, Z.-J. Li, Y. Yan, R. Han, H. Liu, M. Ma, Genome-wide analysis of the SPL family transcription factors and their responses to abiotic stresses in maize, Plant Gene 6 (2016) 1–12, https://doi.org/10.1016/j.plgene.2016.03.003.

F.J. Molina-Hidalgo, M. Vazquez-Vilar, L. D'Andrea, O.C. Demurtas, P. Fraser, G. Giuliano, R. Bock, D. Orzáez, A. Goossens, Engineering Metabolism in Nicotiana Species: A Promising Future, Trends Biotechnol. 39 (9) (2021) 901–913, https://doi.org/10.1016/j.tibtech.2020.11.012.

P. Moreno, S. Fexova, N. George, J.R. Manning, Z. Miao, S. Mohammed, A. Muñoz-Pomer, A. Fullgrabe, Y. Bi, N. Bush, H. Iqbal, U. Kumbham, A. Solovyev, L. Zhao, A. Prakash, D. García-Seisdedos, D.J. Kundu, S. Wang, M. Walzer, I. Papatheodorou, Expression Atlas update: Gene and protein expression in multiple species, Nucleic Acids Res. 50 (D1) (2022) D129–D140, https://doi.org/10.1093/nar/gkab1030.

E. Moreno-Giménez, S. Selma, C. Calvache, D. Orzáez, GB_SynP: A Modular dCas9-Regulated Synthetic Promoter Collection for Fine-Tuned Recombinant Gene Expression in Plants, ACS Synth. Biol. 11 (9) (2022) 3037–3048, https://doi.org/10.1021/acssynbio.2c00238.

MOTIF: Searching Protein Sequence Motif s, n.d., Retrieved January 13, 2023, from https://www.genome.jp/tools/motif/.

M.G. Murray, W.F. Thompson, Rapid isolation of high molecular weight plant DNA, Nucleic Acids Res. 8 (19) (1980), https://doi.org/10.1093/nar/8.19.4321.

L.-T. Nguyen, H.A. Schmidt, A. von Haeseler, B.Q. Minh, IQ-TREE: A fast and effective stochastic algorithm for estimating maximum-likelihood phylogenies, Mol. Biol. Evol. 32 (1) (2015) 268–274, https://doi.org/10.1093/molbev/msu300.

Nicotiana benthamiana Genome & Wild Transcriptome Site, n.d., PW . Retrieved January 13, 2023, from https://www.nbenth.com/.

M.S. Padmanabhan, S. Ma, T.M. Burch-Smith, K. Czymmek, P. Huijser, S.P. Dinesh-Kumar, Novel positive regulatory role for the SPL6 transcription factor in the N TIR-NB-LRR receptor-mediated plant innate immunity, PLoS Pathog. 9 (3) (2013), e1003235, https://doi.org/10.1371/journal.ppat.1003235.

F. Pan, Y. Wang, H. Liu, M. Wu, W. Chu, D. Chen, Y. Xiang, Genome-wide identification and expression analysis of SBP-like transcription factor genes in Moso Bamboo (Phyllostachys edulis, BMC Genom. 18 (1) (2017) 486, https://doi.org/10.1186/s12864-017-3882-4.

M. Pertea, G.M. Pertea, C.M. Antonescu, T.-C. Chang, J.T. Mendell, S.L. Salzberg, StringTie enables improved reconstruction of a transcriptome from RNA-seq reads, Nature Biotechnology 33 (3) (2015) 290–295, https://doi.org/10.1038/nbt.3122.

J.C. Preston, L.C. Hileman, Functional Evolution in the Plant SQUAMOSA-PROMOTER BINDING PROTEIN-LIKE (SPL) Gene Family, Front. Plant Sci. 4 (2013) 80, https://doi.org/10.3389/fpls.2013.00080.

Ranawaka, B., An, J., Lorenc, M.T., Jung, H., Sulli, M., Aprea, G., Roden, S., Hayashi, S., Cooper, T., LeBlanc, Z., Llaca, V., Orzaez, D., Bombarely, A., Bally, J., Winefield, C., Giuliano, G., & Waterhouse, P.M. (2022). A multi-omic Nicotiana benthamiana resource for fundamental research and biotechnology (p. 2022.12.30.521993). bioRxiv. https://doi.org/10.1101/2022.12.30.521993.

M.D. Robinson, D.J. McCarthy, G.K. Smyth, edgeR: A Bioconductor package for differential expression analysis of digital gene expression data, Bioinforma. (Oxf., Engl.) 26 (1) (2010) 139–140, https://doi.org/10.1093/bioinformatics/btp616.

K. Rogers, X. Chen, Biogenesis, turnover, and mode of action of plant microRNAs, Plant Cell 25 (7) (2013) 2383–2399, https://doi.org/10.1105/tpc.113.113159.

M. Salinas, S. Xing, S. Höhmann, R. Berndtgen, P. Huijser, Genomic organization, phylogenetic comparison and differential expression of the SBP-box family of

transcription factors in tomato, Planta 235 (6) (2012) 1171–1184, https://doi.org/10.1007/s00425-011-1565-y.
Sayers, E.W., Bolton, E.E., Brister, J.R., Canese, K., Chan, J., Comeau, D.C., Connor, R., Funk, K., Kelly, C., Kim, S., Madej, T., Marchler-Bauer, A., Lanczycki, C., Lathrop, S., Lu, Z., Thibaud-Nissen, F., Murphy, T., Phan, L., Skripchenko, Y., … Sherry, S.T. (2022). Database resources of the national center for biotechnology information. Nucleic Acids Research, 50(D1), D20–D26. https://doi.org/10.1093/nar/gkab1112.
M. Schiavinato, M. Marcet-Houben, J.C. Dohm, T. Gabaldón, H. Himmelbauer, Parental origin of the allotetraploid tobacco Nicotiana benthamiana, Plant J.: Cell Mol. Biol. 102 (3) (2020) 541–554, https://doi.org/10.1111/tpj.14648.
S. Schwarz, A.V. Grande, N. Bujdoso, H. Saedler, P. Huijser, The microRNA regulated SBP-box genes SPL9 and SPL15 control shoot maturation in Arabidopsis, Plant Mol. Biol. 67 (1) (2008) 183–195, https://doi.org/10.1007/s11103-008-9310-z.
Sheludko, Y. v, Sindarovska, Y. r, Gerasymenko, I. m, Bannikova, M. a., & Kuchuk, N. v. (2007). Comparison of several Nicotiana species as hosts for high-scale Agrobacterium-mediated transient expression. Biotechnology and Bioengineering, 96(3), 608–614. https://doi.org/10.1002/bit.21075.
N. Sierro, J.N.D. Battey, S. Ouadi, N. Bakaher, L. Bovet, A. Willig, S. Goepfert, M. C. Peitsch, N.V. Ivanov, The tobacco genome sequence and its comparison with those of tomato and potato, Nat. Commun. 5 (2014) 3833, https://doi.org/10.1038/ncomms4833.
G.S.C. Slater, E. Birney, Automated generation of heuristics for biological sequence comparison, BMC Bioinforma. 6 (2005) 31, https://doi.org/10.1186/1471-2105-6-31.
A. Song, T. Gao, D. Wu, J. Xin, S. Chen, Z. Guan, H. Wang, L. Jin, F. Chen, Transcriptome-wide identification and expression analysis of chrysanthemum SBP-like transcription factors, Plant Physiol. Biochem.: PPB 102 (2016) 10–16, https://doi.org/10.1016/j.plaphy.2016.02.009.
Stone, J.M., Liang, X., Nekl, E.R., & Stiers, J.J. (2005). Arabidopsis AtSPL14, a plant-specific SBP-domain transcription factor, participates in plant development and sensitivity to fumonisin B1. The Plant Journal: For Cell and Molecular Biology, 41 (5), 744–754. https://doi.org/10.1111/j.1365–313X.2005.02334.x.
Synthego, n.d., Synthego. Retrieved January 13, 2023, from https://ice.synthego.com/#/.
R.K. Tripathi, P. Bregitzer, J. Singh, Genome-wide analysis of the SPL/miR156 module and its interaction with the AP2/miR172 unit in barley, Sci. Rep. 8 (1) (2018) 7085, https://doi.org/10.1038/s41598-018-25349-0.
U.S. Unte, A.-M. Sorensen, P. Pesaresi, M. Gandikota, D. Leister, H. Saedler, P. Huijser, SPL8, an SBP-box gene that affects pollen sac development in Arabidopsis, Plant Cell 15 (4) (2003) 1009–1019, https://doi.org/10.1105/tpc.010678.
T.W.J.M. van Herpen, K. Cankar, M. Nogueira, D. Bosch, H.J. Bouwmeester, J. Beekwilder, Nicotiana benthamiana as a Production Platform for Artemisinin Precursors, PLOS ONE 5 (12) (2010), e14222, https://doi.org/10.1371/journal.pone.0014222.
M. Vazquez-Vilar, M. Gandía, V. García-Carpintero, E. Marqués, A. Sarrion-Perdigones, L. Yenush, J. Polaina, P. Manzanares, J.F. Marcos, D. Orzaez, Multigene Engineering by GoldenBraid Cloning: From Plants to Filamentous Fungi and Beyond, Curr. Protoc. Mol. Biol. 130 (1) (2020), e116, https://doi.org/10.1002/cpmb.116.
Vazquez-Vilar, M., Garcia-Carpintero, V., Selma, S., Bernabé-Orts, J.M., Sanchez-Vicente, J., Salazar-Sarasua, B., Ressa, A., de Paola, C., Ajenjo, M., Quintela, J.C., Fernández-del-Carmen, A., Granell, A., & Orzáez, D. (2021). The GB4.0 Platform, an All-In-One Tool for CRISPR/Cas-Based Multiplex Genome Engineering in Plants. Frontiers in Plant Science, 12, 689937. https://doi.org/10.3389/fpls.2021.689937.
H. Wang, H. Wang, The miR156/SPL Module, a Regulatory Hub and Versatile Toolbox, Gears up Crops for Enhanced Agronomic Traits, Mol. Plant 8 (5) (2015) 677–688, https://doi.org/10.1016/j.molp.2015.01.008.
J. Wang, H. Yu, G. Xiong, Z. Lu, Y. Jiao, X. Meng, G. Liu, X. Chen, Y. Wang, J. Li, Tissue-Specific Ubiquitination by IPA1 INTERACTING PROTEIN1 Modulates IPA1 Protein Levels to Regulate Plant Architecture in Rice, Plant Cell 29 (4) (2017) 697–707, https://doi.org/10.1105/tpc.16.00879.
Wu, G., & Poethig, R.S. (2006). Temporal regulation of shoot development in Arabidopsis thaliana by miR156 and its target SPL3. Development (Cambridge, England), 133(18), 3539–3547. https://doi.org/10.1242/dev.02521.
Xie, K., Minkenberg, B., & Yang, Y. (2015). Boosting CRISPR/Cas9 multiplex editing capability with the endogenous tRNA-processing system. Proceedings of the National Academy of Sciences of the United States of America, 112(11), 3570–3575. https://doi.org/10.1073/pnas.1420294112.
S. Xing, M. Salinas, S. Höhmann, R. Berndtgen, P. Huijser, MiR156-targeted and nontargeted SBP-box transcription factors act in concert to secure male fertility in Arabidopsis, Plant Cell 22 (12) (2010) 3935–3950, https://doi.org/10.1105/tpc.110.079343.
M. Xu, T. Hu, J. Zhao, M.-Y. Park, K.W. Earley, G. Wu, L. Yang, R.S. Poethig, Developmental Functions of miR156-Regulated SQUAMOSA PROMOTER BINDING PROTEIN-LIKE (SPL) Genes in Arabidopsis thaliana, PLoS Genet. 12 (8) (2016), e1006263, https://doi.org/10.1371/journal.pgen.1006263.
H. Yamasaki, M. Hayashi, M. Fukazawa, Y. Kobayashi, T. Shikanai, SQUAMOSA Promoter Binding Protein-Like7 Is a Central Regulator for Copper Homeostasis in Arabidopsis, Plant Cell 21 (1) (2009) 347–361, https://doi.org/10.1105/tpc.108.060137.
S. Yang, M. Overlander-Chen, C.H. Carlson, J.D. Fiedler, A SQUAMOSA promoter binding protein-like transcription factor controls crop ideotype for high productivity in barley, Plant Direct 6 (9) (2022), e450, https://doi.org/10.1002/pld3.450.
Z. Yang, X. Wang, S. Gu, Z. Hu, H. Xu, C. Xu, Comparative study of SBP-box gene family in Arabidopsis and rice, Gene 407 (1–2) (2008) 1–11, https://doi.org/10.1016/j.gene.2007.02.034.
N. Yu, W.-J. Cai, S. Wang, C.-M. Shan, L.-J. Wang, X.-Y. Chen, Temporal control of trichome distribution by microRNA156-targeted SPL genes in Arabidopsis thaliana, Plant Cell 22 (7) (2010) 2322–2335, https://doi.org/10.1105/tpc.109.072579.
N. Yu, Q.-W. Niu, K.-H. Ng, N.-H. Chua, The role of miR156/SPLs modules in Arabidopsis lateral root development, Plant J.: Cell Mol. Biol. 83 (4) (2015) 673–685, https://doi.org/10.1111/tpj.12919.
R.-F. Zeng, J.-J. Zhou, S.-R. Liu, Z.-M. Gan, J.-Z. Zhang, C.-G. Hu, Genome-Wide Identification and Characterization of SQUAMOSA-Promoter-Binding Protein (SBP) Genes Involved in the Flowering Development of Citrus Clementina, Biomolecules 9 (2) (2019), E66, https://doi.org/10.3390/biom9020066.
T. Zhang, J. Wang, C. Zhou, The role of miR156 in developmental transitions in Nicotiana tabacum, Sci. China Life Sci. 58 (3) (2015) 253–260, https://doi.org/10.1007/s11427-015-4808-5.
Y. Zhang, S. Schwarz, H. Saedler, P. Huijser, SPL8, a local regulator in a subset of gibberellin-mediated developmental processes in Arabidopsis, Plant Mol. Biol. 63 (3) (2007) 429–439, https://doi.org/10.1007/s11103-006-9099-6.
Q. Zhou, S. Zhang, F. Chen, B. Liu, L. Wu, F. Li, J. Zhang, M. Bao, G. Liu, Genome-wide identification and characterization of the SBP-box gene family in Petunia, BMC Genom. 19 (1) (2018) 193, https://doi.org/10.1186/s12864-018-4537-9.